

# PhD Thesis Defense



## Estudio de la Interacción de Flujos Múltiples de Fuentes Astrofísicas, Aplicada a los Proplyds Clásicos de la Nebulosa de Orión

Presents: M.C Jorge Alejandro Tarango Yong

PhD Advisor: Dr. William Henney

Tutorial Committee: Dr. Javier Ballesteros, Dr. Luis Zapata

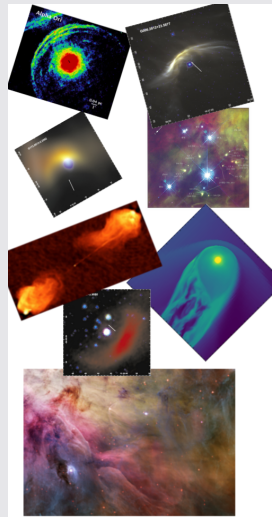
October 1, 2018

# Index

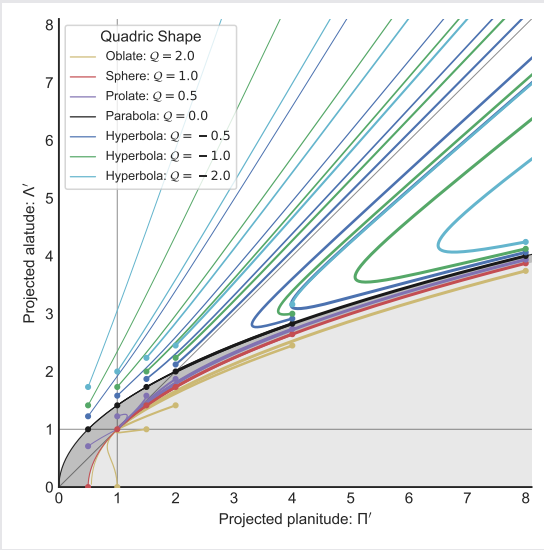
- 1 Introduction**
- 2 Bow Shocks in the ISM**
- 3 Orion Nebula**
- 4 Fundamental Concepts**
- 5 Thin Shell Model**
- 6 Results Obtained to the Classical Proplyds of Orion Nebula**
- 7 Summary and Conclusions**

# Motivation of this work

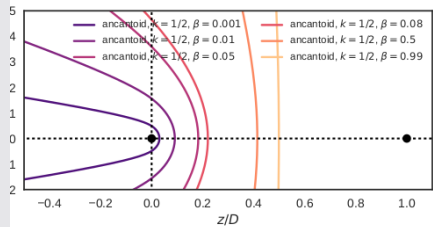
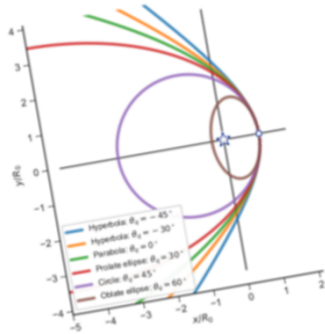
Bow shocks occur in many kinds of astrophysical scenarios, from galactic to planetary scales. In this work we develop a mathematical tool for characterizing cylindrically symmetric, geometrically thin and optically thin bow shocks based into their geometrical shape and how is oriented respect the plane of sky.



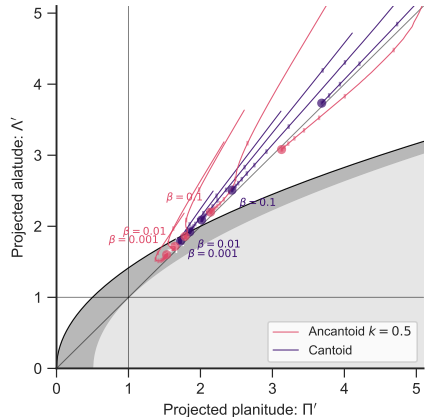
We called it the  $\Lambda'$  –  $\Pi'$  diagram (Tarango Yong & Henney, 2018).



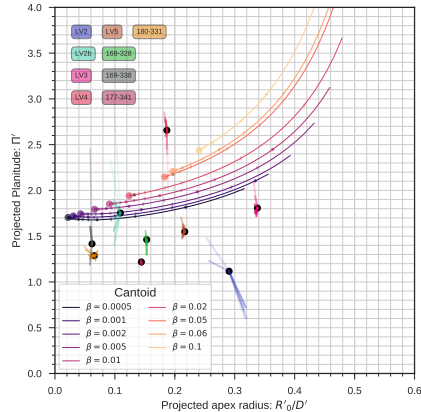
Then we apply this tool to the simplest mathematical surfaces: the quadrics of revolution (Goldman, 1983; Gfrerrer & Zsombor-Murray, 2009) and to a simple model for winds interaction: the Thin Shell Model (Canto et al., 1996).



Then we apply this tool to the simplest mathematical surfaces: the quadrics of revolution (Goldman, 1983; Gfrerrer & Zsombor-Murray, 2009) and to a simple model for winds interaction: the Thin Shell Model (Canto et al., 1996).



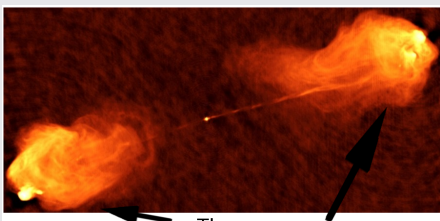
And finally compare the thin shell model against observations of the classical proplyds of the Trapezium in the core of the Orion Nebula in a similar diagram.



# Bow Shocks in the ISM

Bow shocks are emission arcs produced when some fluid interacts at supersonic speeds with another object. Some astrophysical examples seen in the Interstellar Medium (ISM) are:

- **Jets Surface Work**
- Magnetosphere interaction with stellar wind
- Stellar Bow shocks
  - AGB stars and red supergiants
  - Runaway O stars
  - Proplyds
  - T Tauri stars
  - Neutron stars



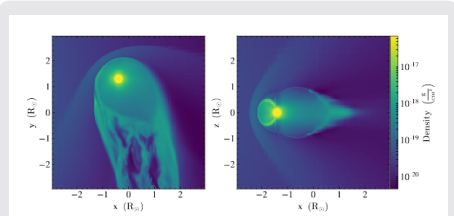
These ones

Cygnus A (Perley et al., 1984)

# Bow Shocks in the ISM

Bow shocks are emission arcs produced when some fluid interacts at supersonic speeds with another object. Some astrophysical examples seen in the Interstellar Medium (ISM) are:

- Jets Surface Work
- **Magnetosphere interaction with stellar wind**
- Stellar Bow shocks
  - AGB stars and red supergiants
  - Runaway O stars
  - Proplyds
  - T Tauri stars
  - Neutron stars

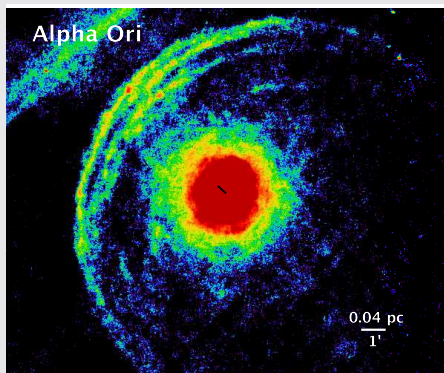


Density of material flowing from a Hot Jupiter through magnetosphere interacting with stellar wind (Daley-Yates & Stevens, 2018).

# Bow Shocks in the ISM

Bow shocks are emission arcs produced when some fluid interacts at supersonic speeds with another object. Some astrophysical examples seen in the Interstellar Medium (ISM) are:

- Jets Surface Work
- Magnetosphere interaction with stellar wind
- Stellar Bow shocks
  - **AGB stars and red supergiants**
  - Runaway O stars
  - Proplyds
  - T Tauri stars
  - Neutron stars

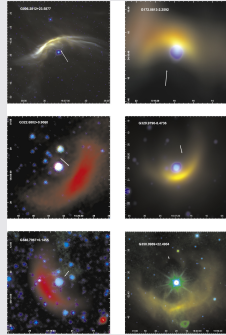


Observation of a “Fermata” type bow shock at  $70 \mu\text{m}$  produced by the interaction of the strong wind of a red supergiant ( $\alpha$  Ori) with the ISM (Cox et al., 2012).

# Bow Shocks in the ISM

Bow shocks are emission arcs produced when some fluid interacts at supersonic speeds with another object. Some astrophysical examples seen in the Interstellar Medium (ISM) are:

- Jets Surface Work
- Magnetosphere interaction with stellar wind
- Stellar Bow shocks
  - AGB stars and red supergiants
  - **Runaway O stars**
  - Proplyds
  - T Tauri stars
  - Neutron stars

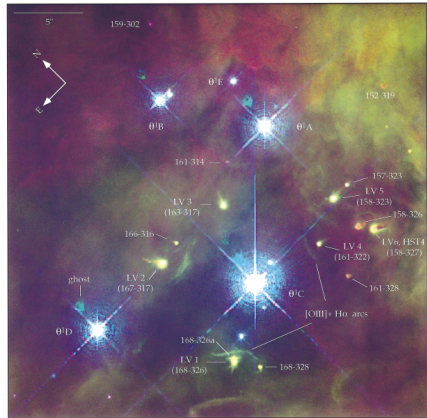


Observations of prototypical examples of “Bow shock nebulae” by Spitzer or WISE produced by runaway stars interacting with the ISM (red: 20 or 22  $\mu$ m, green: 8 or 12  $\mu$ m, blue: 4.5  $\mu$ m)(Kobulnicky et al., 2016).

# Bow Shocks in the ISM

Bow shocks are emission arcs produced when some fluid interacts at supersonic speeds with another object. Some astrophysical examples seen in the Interstellar Medium (ISM) are:

- Jets Surface Work
- Magnetosphere interaction with stellar wind
- Stellar Bow shocks
  - AGB stars and red supergiants
  - Runaway O stars
  - **Proplyds**
  - T Tauri stars
  - Neutron stars



The Classical proplyds in the core of the trapezium in Orion Nebula also show a bow shock by the HST (red is [N II], green is H<sub>α</sub> and blue is [O I]) (Bally et al., 1998).

# Orion Nebula

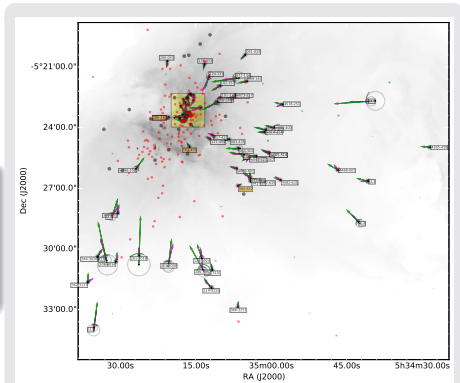
The Orion Nebula is the nearest H II region ( $\sim 414$  pc, Menten et al. (2007)), where massive star formation can be studied with high resolution observations.



[www.hubblesite.org](http://www.hubblesite.org)

# Proplyds in Orion Nebula

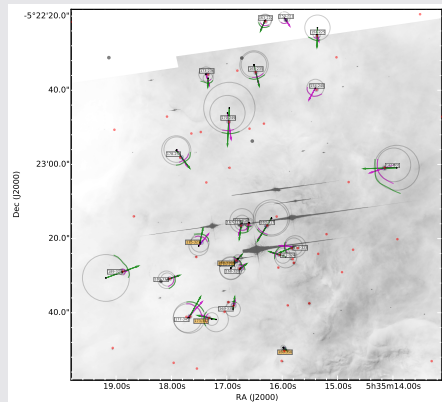
About 70 arcs have been detected within Orion Nebula (Gutiérrez-Soto, 2015), many of them are produced by proplyds.



Map of bow shocks in Orion Nebula  
(Gutiérrez-Soto, 2015)

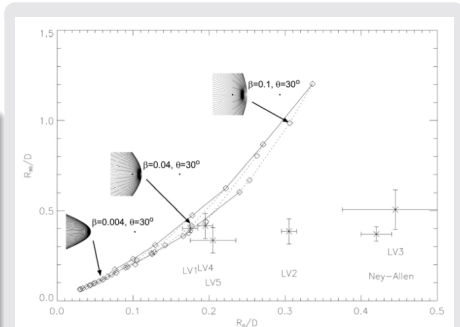
# Proplyds in Orion Nebula

About 70 arcs have been detected within Orion Nebula (Gutiérrez-Soto, 2015), many of them are produced by proplyds.



Map of bow shocks in Orion Nebula (Trapezium zoomed) (Gutiérrez-Soto, 2015)

Some of the nearest proplyds to  $\theta^1$  Ori C were previously observed by Bally et al. (1998) (slide ▶ 10) and Roberto et al. (2005) in mid infrared and their shape analyzed using the Thin Shell Model from (Canto et al., 1996), but some proplyds don't fit at all.



Apparent shape of some proplyds (in black points) compared with the thin shell model of (Canto et al., 1996) (open dots and lines) in a  $R_{90}/D$  vs  $R_0/D$  diagram (Roberto et al., 2005).

Isotropic



$k = 0, \xi = 1.0$



$k = 0.5, \xi = 0.8$



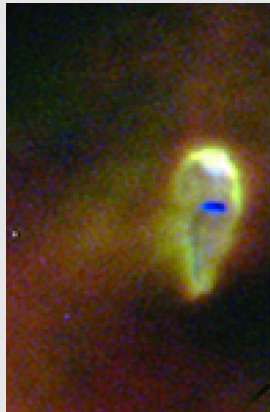
$k = 3, \xi = 0.4$



This motivated us to extend Canto et al. (1996) model to include non isotropic winds.

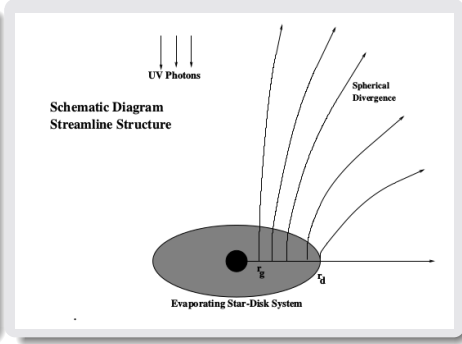
# Photoevaporated wind in proplyds

Proplyds are bright structures with cometary shape which are the result of the photoevaporation of a protoplanetary disk (hence the name) due to a strong source of ultraviolet radiation (e.g a massive star).

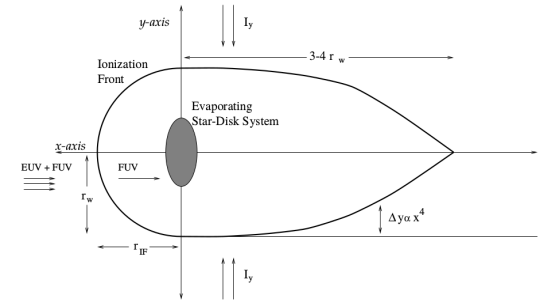


HST10 is the archetypical example of a proplyd. Image taken with the HST (red: F656N filter, green: F658N, blue: F631N filter, Tsamis et al. (2013)).

The incident UV radiation photoevaporates the gas in the protoplanetary disk, which becomes a spherical flow due to pressure gradients. Only the gas located at  $r > r_g = \frac{GM_*}{a^2}$  (where  $M_*$  is the mass of the central star and  $a$  is the speed of sound of the gas) can escape from the disk.



The head is shaped by the incident UV radiation from the massive star, forming a D type Ionization Front, while the tail is shaped by diffuse and ionizing radiation.



(Johnstone et al., 1998)

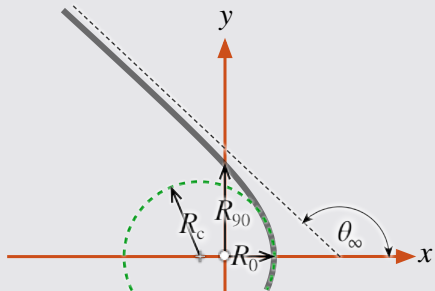


# General Considerations

# Planitude and Alatitude

To characterize the shape of a given bow shock we use a set of parameters:

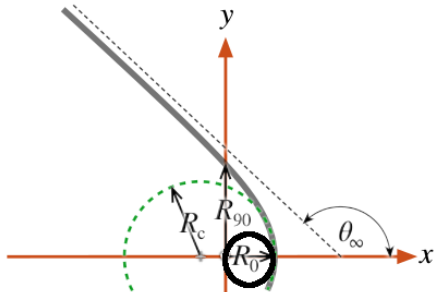
- The radius at the apex, called  $R_0$ , which gives us the bow shock physical scale, and is computed as the minimum of  $R(\theta)$
- The asymptotic angle  $\theta_\infty$  of the far wings (which usually is not measurable)
- The planitude  $\Pi \equiv R_c/R_0$ , which measures how flat is the apex
- The alatitude  $\Lambda \equiv R_{90}/R_0$ , which measures how open the wings are



# Planitude and Alatitude

To characterize the shape of a given bow shock we use a set of parameters:

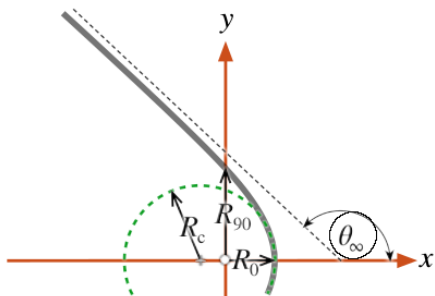
- **The radius at the apex, called  $R_0$ , which gives us the bow shock physical scale, and is computed as the minimum of  $R(\theta)$**
- The asymptotic angle  $\theta_\infty$  of the far wings (which usually is not measurable)
- The planitude  $\Pi \equiv R_c/R_0$ , which measures how flat is the apex
- The alatitude  $\Lambda \equiv R_{90}/R_0$ , which measures how open the wings are



# Planitude and Alatitude

To characterize the shape of a given bow shock we use a set of parameters:

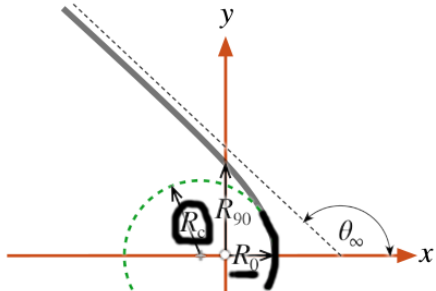
- The radius at the apex, called  $R_0$ , which gives us the bow shock physical scale, and is computed as the minimum of  $R(\theta)$
- **The asymptotic angle  $\theta_\infty$  of the far wings (which usually is not measurable)**
- The planitude  $\Pi \equiv R_c/R_0$ , which measures how flat is the apex
- The alatitude  $\Lambda \equiv R_{90}/R_0$ , which measures how open the wings are



# Planitude and Alatitude

To characterize the shape of a given bow shock we use a set of parameters:

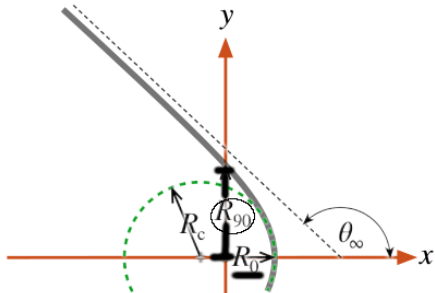
- The radius at the apex, called  $R_0$ , which gives us the bow shock physical scale, and is computed as the minimum of  $R(\theta)$
- The asymptotic angle  $\theta_\infty$  of the far wings (which usually is not measurable)
- **The planitude  $\Pi \equiv R_c/R_0$ , which measures how flat is the apex**
- The alatitude  $\Lambda \equiv R_{90}/R_0$ , which measures how open the wings are



# Planitude and Alatitude

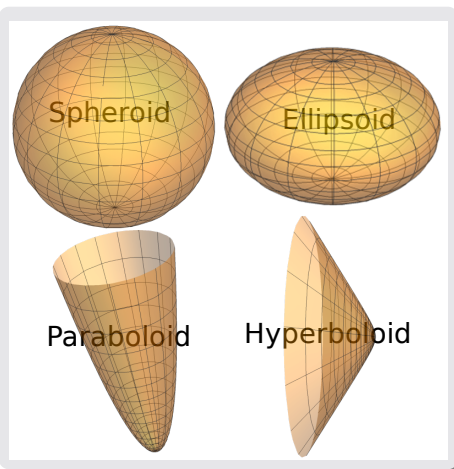
To characterize the shape of a given bow shock we use a set of parameters:

- The radius at the apex, called  $R_0$ , which gives us the bow shock physical scale, and is computed as the minimum of  $R(\theta)$
- The asymptotic angle  $\theta_\infty$  of the far wings (which usually is not measurable)
- The planitude  $\Pi \equiv R_c/R_0$ , which measures how flat is the apex
- **The alatitude  $\Lambda \equiv R_{90}/R_0$ , which measures how open the wings are**



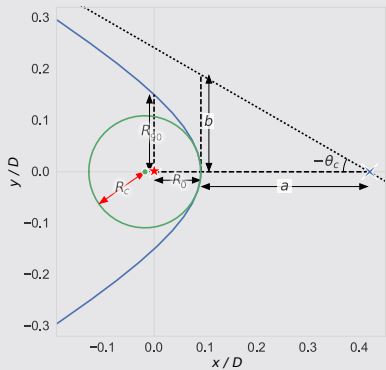
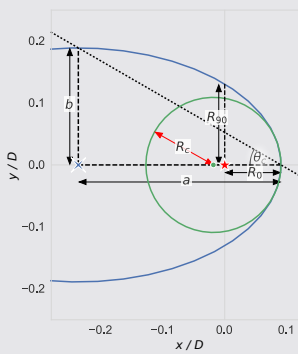
# Quadrics of Revolution

Quadrics of Revolution are the surfaces of revolution of conic sections. May be a good and useful approximation to more complex surfaces



# Quadratics of Revolution: basic definitions

Our conic section symmetry axis is aligned with the  $x$  axis, and the center is displaced from the origin by distance called  $x_0$ . The physical scale of the conic section is set using the semi-major and semi-minor axis  $a$  and  $b$ .



# Quadratics of Revolution: basic definitions

## Parametrization

$$x = x_0 + \sigma a \mathcal{C}(t) \quad (1)$$

$$y = b \mathcal{S}(t) \quad (2)$$

$$\tan \theta = \frac{b \mathcal{S}(t)}{x_0 + \sigma a \mathcal{C}(t)} \quad (3)$$

$$R = \left[ (x_0 + \sigma a \mathcal{C}(t))^2 + b^2 \mathcal{S}^2(t) \right]^{1/2} \quad (4)$$

where:

$$t \forall \mathbb{R} \quad (5)$$

$$\mathcal{C}(t), \mathcal{S}(t) = \begin{cases} \cos t, \sin t & \text{ellipses} \\ \cosh t, \sinh t & \text{hyperbolas} \end{cases} \quad (6)$$

$$\sigma = \begin{cases} +1 & \text{ellipses} \\ -1 & \text{hyperbolas} \end{cases} \quad (7)$$

$$x_0 = R_0 - \sigma a \quad (8)$$

# Quadratics of Revolution: basic definitions

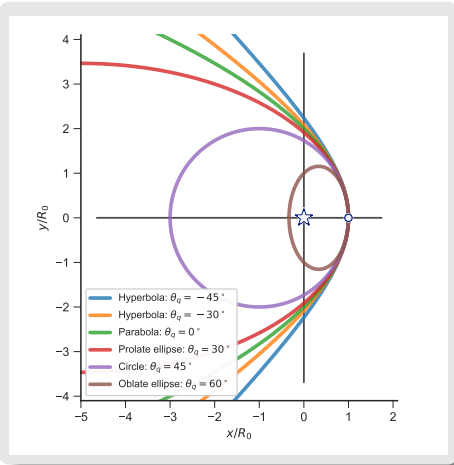
The eccentricity is replaced with the quadratics parameter  $\mathcal{Q}$  defined as:

$$\mathcal{Q} = \sigma \frac{b^2}{a^2} \quad (9)$$

Or the angle  $\theta_q$ :

$$\tan \theta_q = \sigma \frac{b}{a} \quad (10)$$

Positive values of  $\mathcal{Q}$  are associated with closed curves (i.e. ellipsoids), and  $\mathcal{Q} \leq 0$  are associated with open curves.



# Quadrics of Revolution: basic definitions

The parameters set  $(a, x_0, \mathcal{Q})$  is enough to characterize the curve, but for future applications the set  $(R_0, \Pi, \Lambda)$  is more useful. So, the transformation between the two sets is given by:

$$R_0 = x_0 + \sigma a \quad (11)$$

$$\Pi = \frac{a\mathcal{Q}}{a + \sigma x_0} \quad (12)$$

$$\Lambda = \left( \mathcal{Q} \frac{a - \sigma x_0}{a + \sigma x_0} \right)^{1/2} \quad (13)$$

Finally, the quadrics parameter (and thus the kind of quadric) may be computed from the planitude and alatitude as follows:

$$\mathcal{Q} = 2\Pi - \Lambda^2 \quad (14)$$

# Projection Onto the Plane of Sky





## References I

- Bally J., Sutherland R. S., Devine D., Johnstone D., 1998, AJ, 116, 293
- Canto J., Raga A. C., Wilkin F. P., 1996, ApJ, 469, 729
- Cox N. L. J., et al., 2012, A&A, 537, A35
- Daley-Yates S., Stevens I. R., 2018, MNRAS, 479, 1194
- Gfrerrer A., Zsombor-Murray P., 2009, Journal for Geometry and Graphics, 13, 131–144
- Goldman R., 1983, IEEE Computer Graphics and Applications, 3, 68–76
- Gutiérrez-Soto L. , 2015, Master's thesis, Universidad Nacional Autónoma de México
- Johnstone D., Hollenbach D., Bally J., 1998, ApJ, 499, 758
- Kobulnicky H. A., et al., 2016, ApJS, 227, 18
- Menten K. M., Reid M. J., Forbrich J., Brunthaler A., 2007, A&A, 474, 515

## References II

- Perley R. A., Dreher J. W., Cowan J. J., 1984, ApJ, 285, L35
- Robberto M., et al., 2005, AJ, 129, 1534
- Tarango Yong J. A., Henney W. J., 2018, MNRAS, 477, 2431
- Tsamis Y. G., Flores-Fajardo N., Henney W. J., Walsh J. R., Mesa-Delgado A., 2013, MNRAS, 430, 3406